# Luminescence Investigation on Ultraviolet-Emitting Rare-Earth-Doped Phosphors Using Synchrotron Radiation

Chien-Hao Huang,[†] Teng-Ming Chen,*[,†] and Bing-Ming Cheng[‡]

[†]Phosphors Research Laboratory and Department of Applied Chemistry, National Chiao Tung University, Hsinchu 30010, Taiwan
[‡]National Synchrotron Radiation Research Center, Hsinchu Science Park, Hsinchu 30076, Taiwan

**ABSTRACT:** Three series of new ultraviolet-emitting $Ca_9Y(PO_4)_7{:}Ln^{3+}$ (Ln = Ce, Gd, Pr) phosphors were synthesized, and their luminescence was investigated. Under vacuum ultraviolet excitation $Ca_9Y(PO_4)_7{:}Ce^{3+}$ phosphors emit UVA light with one broad emission centered at 346 nm, on account of the $5d^1 \rightarrow 4f^1$ transition of $Ce^{3+}$ ions; the optimal doping concentration of these phosphors is 0.2 mol. $Ca_9Y(PO_4)_7{:}Gd^{3+}$ phosphors show a strong $4f^7 \rightarrow 4f^7$ transition and a sharp UVB emission band at 312 nm; the optimal doping concentration of these phosphors is 0.7 mol. The PL spectra of $Ca_9Y(PO_4)_7{:}Pr^{3+}$ show two broad UVC emission bands centered between 230 and 340 nm, owing to the $4f^1 5d^1 \rightarrow 4f^2$ transition of $Pr^{3+}$ ions; the optimal doping concentration of these phosphors is 0.2 mol. Under 172 nm excitation, we found that the luminescence intensity of the UVA-emitting $Ca_9Y(PO_4)_7{:}0.2Ce^{3+}$ is 0.3675 times that of $BaSi_2O_5{:}0.05Pb^{2+}$, that of the UVB-emitting $Ca_9Y(PO_4)_7{:}0.7Gd^{3+}$ is 1.7 times that of $YAl_3(BO_3)_4{:}0.25Gd^{3+}$, and that of the UVC-emitting $Ca_9Y(PO_4)_7{:}0.2Pr^{3+}$ is 1.5 times that of $LaPO_4{:}0.1Pr^{3+}$. The thermal stability investigation indicated that the luminescence decay was only 9.2%, 18.2%, and 10.3% for $Ca_9Y(PO_4)_7{:}0.2Ce^{3+}$, $Ca_9Y(PO_4)_7{:}0.7Gd^{3+}$, and $Ca_9Y(PO_4)_7{:}0.2Pr^{3+}$ at 250 °C relative to that at ambient temperature, respectively. The $Ca_9Y(PO_4)_7{:}Ln^{3+}$ (Ln = Ce, Gd, Pr) phosphors exhibit high emission efficiency and excellent thermal stability.
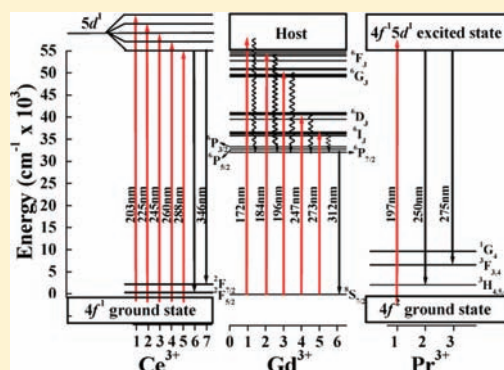
## 1. INTRODUCTION

In recent years, ultraviolet radiation (UVR) has been extensively used in a variety of applications such as examination of counterfeit banknotes and insect traps,[1] production of vitamin $D_3$,[2] and photochemical reactions.[3] It has also been used in medical applications such as treatment of psoriasis,[4] induction of DNA damage,[5] sterilization and disinfection,[6] and delay of ripening.[7] UVR can be generally divided into three categories: ultraviolet A (UVA, 400−320 nm), ultraviolet B (UVB, 320−280 nm), and ultraviolet C (UVC, 280−200 nm). More than 98% of UVA radiation reaches the surface of the earth. Most of the UVB radiation is absorbed by the atmosphere, and only <2% of UVB radiation reaches the surface of the earth. UVC radiation is completely scattered and absorbed by $O_3$, $O_2$, and $N_2$ into the atmospheric layer.[8]

For designing ultraviolet-emitting phosphors, the most suitable activators used are $Ce^{3+}$, $Gd^{3+}$, $Pr^{3+}$, and $Pb^{2+}$ ions. Tian et al.[9] studied the PLE spectra of $GdPO_4{:}Ce^{3+}$ and found that five crystal field splitting components were present at 206, 214, 236, 256, and 274 nm; these components were formed because of the crystal field splitting of $Ce^{3+}$ 5d states in $GdPO_4{:}Ce^{3+}$. Under 155- nm excitation, strong UVA emissions at around 343 nm of $Ce^{3+}$ ($5d^1 \rightarrow 4f^1$) and 311 nm of $Gd^{3+}$ ($^6P_{7/2} \rightarrow {}^8S_{7/2}$) can be observed; this observation implies that the efficient energy is transferred between the host lattice and $Ce^{3+}$. Narrow-band UVB-emitting phosphors of $YAl_3(BO_3)_4{:}Gd^{3+}$ and $LaPO_4{:}$ $Gd^{3+}$,$Pr^{3+}$ have been observed by Yokosawa et al.[10] and Okamoto et al, respectively.[11] They reported that the emission spectra of $YAl_3(BO_3)_4{:}Gd^{3+}$ and $LaPO_4{:}Gd^{3+}$,$Pr^{3+}$ at 313 and 312 nm, respectively, originated from the $^6P_{7/2}$ to $^8S_{7/2}$ transition of $Gd^{3+}$ ions. The authors reported that the emission intensity of $(La_{0.65}Gd_{0.35})_{0.95}Pr_{0.05}PO_4$ is approximately 1.6 times that of $Y_{0.75}Gd_{0.25}Al_3(BO_3)_4$ under 172 nm excitation. According to Yuan et al.,[12] $NaLaP_2O_7{:}Pr^{3+}$ phosphor shows three excitation bands between 160 and 225 nm; these bands are attributed to the $4f^2 \rightarrow 4f^1 5d^1$ transition of $Pr^{3+}$ ions states. The PL spectra show a moderately strong $4f^1 5d^1 \rightarrow 4f^2$ ($^3H_J$, $^3F_J$, $^1G_4$, $^1D_2$, $^3P_J$, $^1I_6$) transition and broad emission bands. Folkerts et al.[13] described $Pb^{2+}$-doped alkaline earth sulfates and indicated that the PL spectra of $CaSO_4{:}Pb^{2+}$ show a broad emission band and an excitation band with a maximum at 235 and 220 nm owing to the $sp \rightarrow s^2$ ($^3P_{0,1} \rightarrow {}^1S_0$) and $s^2 \rightarrow sp$ transitions of $Pb^{2+}$ ions, respectively.

In this study, the luminescence property, thermal stability, and emission efficiency of UV-emitting $Ca_9Y(PO_4)_7{:}Ln^{3+}$ (Ln = Ce, Gd, Pr) phosphors have been reported. Our results indicated that $Ca_9Y(PO_4)_7{:}Ln^{3+}$ (Ln = Ce, Gd, Pr) phosphors have good thermal stability and high luminous efficiency and, therefore, may serve as promising ultraviolet-radiation phosphors for application in xenon excimer discharge lamps.
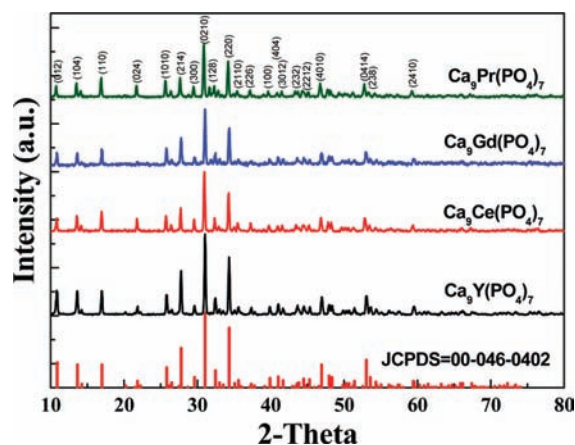
**Figure 1.** Powder XRD patterns of $Ca_9Y(PO_4)_7$, $Ca_9Ce(PO_4)_7$, $Ca_9Gd(PO_4)_7$, and $Ca_9Pr(PO_4)_7$ (JCPDS file no. 00-046-0402).

## 2. EXPERIMENTAL SECTION

**2.1. Materials and Synthesis.** Polycrystalline phosphors of $Ca_9(Y_{1-x}Ce_x)(PO_4)_7$, $Ca_9(Y_{1-y}Gd_y)(PO_4)_7$, and $Ca_9(Y_{1-z}Pr_z)(PO_4)_7$ were prepared using a high-temperature solid-state reaction. Initially, the constituent raw materials $CaCO_3$, $Y_2O_3$ (99.99%), $(NH_4)_2HPO_4$, $CeO_2$ (99.99%), $Gd_2O_3$ (99.99%), and $Pr_2O_3$ (99.99%) (all analytically high purity from Aldrich Chemicals) were weighed in stoichiometric proportions, mixed thoroughly ground in an agate mortar, and then placed in an alumina crucible, which was heated at 1250 °C for 8 h and then cooled slowly to room temperature. The $Ca_9(Y_{1-x}Ce_x)(PO_4)_7$ phosphors were then reduced at 1000 °C for 6 h under a reducing atmosphere of 15% $H_2$/85% $N_2$ in an alumina boat.

**2.2. Materials Characterization.** The phase purity of the as-prepared samples was checked by powder X-ray diffraction (XRD) analysis with a Bruker AXS D8 advanced automatic diffractometer with Cu Kα radiation ($\lambda = 1.5418$ Å) over the angular range $10° \leq 2\theta \leq 80°$, operating at 40 $mA$. The photoluminescence (PL) and photoluminescence excitation (PLE) spectra were recorded upon excitation with vacuum ultraviolet (VUV) radiation, which was dispersed from a high-flux beamline with a 6 m cylindrical grating monochromator (CGM) coupled to the 1.5 GeV storage ring at the National Synchrotron Radiation Research Center (NSRRC) in Taiwan. This CGM beamline spans the energy range 4−40 eV with a resolving power of 40 000; the highest photon flux is about $2 \times 10^{12}$ photons/s. The incident VUV light was conducted through a gold mesh with about 90% transmission; subsequently, the photocurrent of the gold mesh was detected by an electrometer (Keithley 6512) for monitoring and normalization of the beam. To remove the high-order light, the excitation light further transmitted a $CaF_2$ window before being irradiated onto the sample. Emission of the PL was analyzed by a Jobin-Yvon HR320 monochromator with a maximum resolution of 0.04 nm. Finally, the intensity of dispersed PL emission from the sample was detected with a photomultiplier (Hamamatsu R943-02) in photon-counting mode. The variable-temperature PL spectra were carried out with a Jobin-Yvon Spex, model FluoroMax-3 spectrophotometer. The microstructure of phosphor samples was examined using a field emission-type scanning electron microscope (SEM) (S-4800, Hitachi, Japan).

## 3. RESULTS AND DISCUSSION

**3.1. Crystal Structure and Microstructure Investigations.** Figure 1 shows the powder XRD patterns of $Ca_9(Y_{1-x}Ce_x)(PO_4)_7$ (CYP:$x$Ce$^{3+}$; $0 < x \leq 1$), $Ca_9(Y_{1-y}Gd_y)(PO_4)_7$ (CYP:
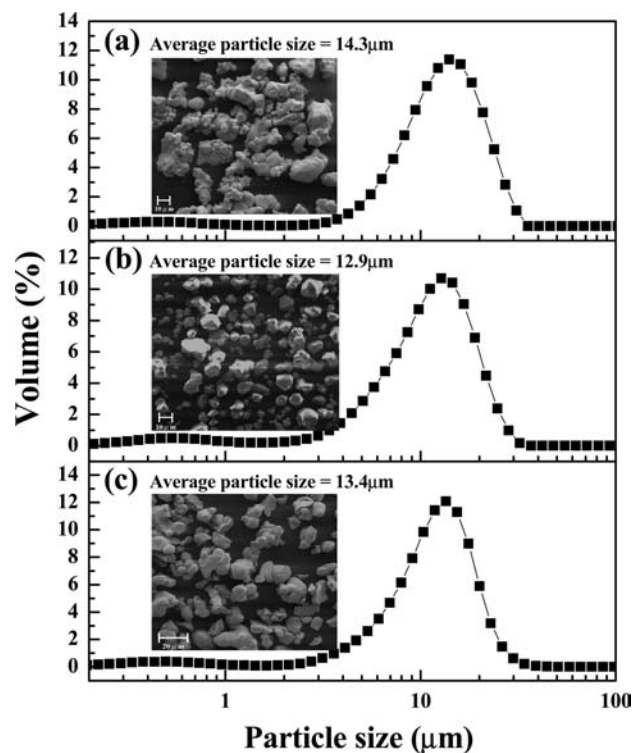


**Figure 2.** Particle size distribution and SEM micrographs of (a) $Ca_9Y(PO_4)_7$:0.2Ce$^{3+}$, (b) $Ca_9Y(PO_4)_7$:0.7Gd$^{3+}$, and (c) $Ca_9Y(PO_4)_7$:0.2Pr$^{3+}$ phosphors.

$y$Gd$^{3+}$; $0 < y \leq 1$)), and $Ca_9(Y_{1-z}Pr_z)(PO_4)_7$ (CYP:$z$Pr$^{3+}$; $0 < z \leq 1$)); all of these patterns agree well with that of the JCPDS file no. 00-046-0402. These results indicate that the $Ca_9Y(PO_4)_7$ structure is retained and has not generated any X-ray detectable impurity to appear even when Y$^{3+}$ ions were all substituted by Ce$^{3+}$ or Gd$^{3+}$ or Pr$^{3+}$ ion. $Ca_9Y(PO_4)_7$ crystallizes[14] as a rhombohedral unit cell with space group $R3c$ (No. 161), lattice constants $a = 10.4442$ Å and $c = 37.324$ Å, cell volume = 3525.89 Å$^3$, and $Z = 6$. The Y$^{3+}$ ion is six coordinate, and the ionic radius of six-coordinated Y$^{3+}$ is 0.9 Å. However, the ionic radii of six-coordinated Ce$^{3+}$, Gd$^{3+}$, Pr$^{3+}$ are 1.01, 0.938, and 0.99 Å, respectively. On account of the matching of ionic radii and isovalent substitution, the Ce$^{3+}$, Gd$^{3+}$, and Pr$^{3+}$ ions are expected to occupy the Y$^{3+}$ ions sites in the $Ca_9Y(PO_4)_7$ host. Shown in Figure 2 are the distribution of particle size and SEM images of $Ca_9Y(PO_4)_7$:0.2Ce$^{3+}$, $Ca_9Y(PO_4)_7$:0.7Gd$^{3+}$, and $Ca_9Y(PO_4)_7$:0.2Pr$^{3+}$ phosphors. The particle size distribution of UVR phosphors was found to vary from 1 to 35 $\mu$m, and the averge particle sizes of $Ca_9Y(PO_4)_7$:0.2Ce$^{3+}$, $Ca_9Y(PO_4)_7$:0.7Gd$^{3+}$, and $Ca_9Y(PO_4)_7$:0.2Pr$^{3+}$ phosphors are about 14.3, 12.9, and 13.4 $\mu$m. The inset of Figure 2 shows SEM micrographs of the UVR phosphors, which reveals that particles are aggregated and the shape is irregular.

**3.2. Photoluminescence and Energy Level Diagrams.** Figures 3 and 4 show the PL/PLE spectra and proposed energy level schemes of $Ca_9Y(PO_4)_7$, $Ca_9Y(PO_4)_7$:Ce$^{3+}$, $Ca_9Y(PO_4)_7$:Gd$^{3+}$, and $Ca_9Y(PO_4)_7$:Pr$^{3+}$ phosphors. Figure 3a shows the excitation and emission spectra of the $Ca_9Y(PO_4)_7$ host; as shown in this figure, broad absorption and emission bands at around 120−230 and 300−600 nm, respectively, are attributed to the self-emission of the $Ca_9Y(PO_4)_7$ host. Under 225 nm excitation,

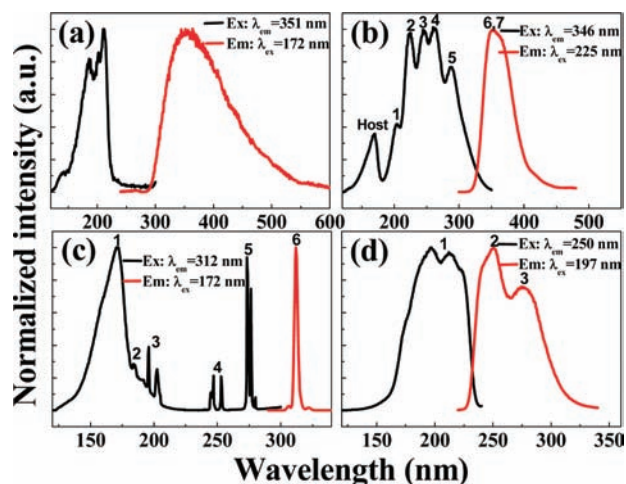**Figure 3.** Excitation (black line) and emission spectra (red line) of (a) $Ca_9Y(PO_4)_7$, (b) $Ca_9Y(PO_4)_7:Ce^{3+}$, (c) $Ca_9Y(PO_4)_7:Gd^{3+}$, and (d) $Ca_9Y(PO_4)_7:Pr^{3+}$ phosphors.
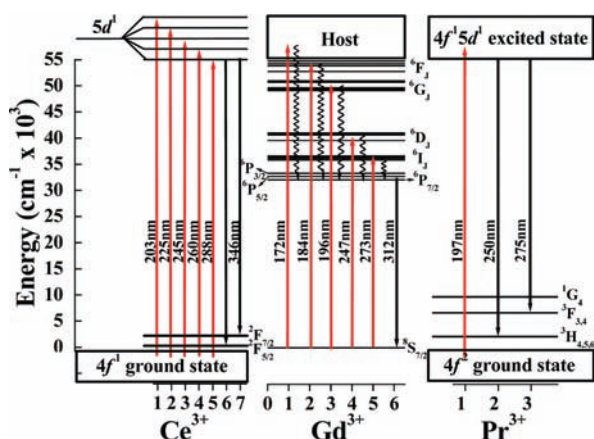


**Figure 4.** Energy level scheme of $Ca_9Y(PO_4)_7:Ce^{3+}$, $Ca_9Y(PO_4)_7:Gd^{3+}$, and $Ca_9Y(PO_4)_7:Pr^{3+}$ phosphors.

$Ca_9Y(PO_4)_7:Ce^{3+}$ phosphors emit UVA light in the form of one broad emission band centered at 346 nm, owing to the $5d^1 \rightarrow 4f^1$ transition of $Ce^{3+}$ ions.[15] The PLE spectra contain several bands from 180 to 350 nm. These bands centered at 203, 225, 245, 260, and 288 nm are attributed to the crystal field splitting of $Ce^{3+}$ 5d states[12] and are shown in Figure 3b. $Ca_9Y(PO_4)_7:Gd^{3+}$ phosphors show a strong $4f^7 \rightarrow 4f^7$ transition and a sharp UVB emission band at around 312 nm, which is attributed to the $^6P_{7/2} \rightarrow {}^8S_{7/2}$ transition of $Gd^{3+}$ ions.[16] There is a single broad band and four excitation bands of $Ca_9Y(PO_4)_7:Gd^{3+}$ between 120 and 280 nm centered at 172, 184, 196, 247, and 273 nm. These bands can be ascribed to the transitions from the ground state to the host and the transition of $^8S_{7/2}$ to $^6F_J$, $^6G_J$, $^6D_J$, and $^6I_{11/2}$,[17] as shown in Figure 3c. The excitation spectra of $Ca_9Y(PO_4)_7:Pr^{3+}$ phosphors show a broad absorption band from 120 to 240 nm, which is attributed to the dipole-allowed $4f^2 \rightarrow 4f^1 5d^1$ transition of $Pr^{3+}$ ions.[18] The PL spectra show two broad UVC emission bands at 230−340 nm, centered at 250 and 275 nm. These bands are attributed to the $4f^1 5d^1 \rightarrow 4f^2$ transition of $Pr^{3+}$ ions,[19] as shown in Figure 3d. On the other hand, in the case of $Ca_9Y(PO_4)_7:zPr^{3+}$ phosphors, we observed a very weak set of 4f−4f transitions and a sharp emission band at 490 nm under 172 nm excitation.



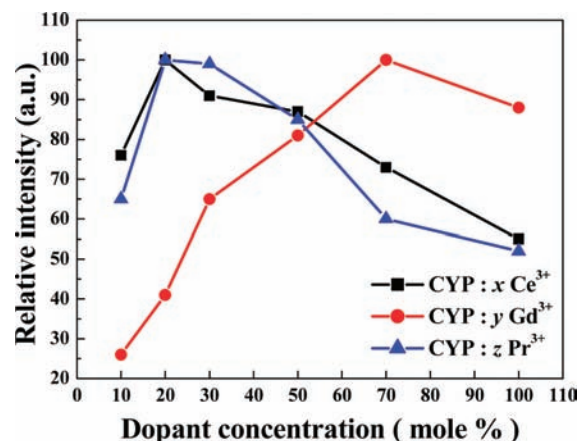**Figure 5.** Concentration dependence of the relative PL intensity of $Ca_9Y(PO_4)_7:xCe^{3+}$, $Ca_9Y(PO_4)_7:yGd^{3+}$, and $Ca_9Y(PO_4)_7:zPr^{3+}$ phosphors under 172 nm excitation.
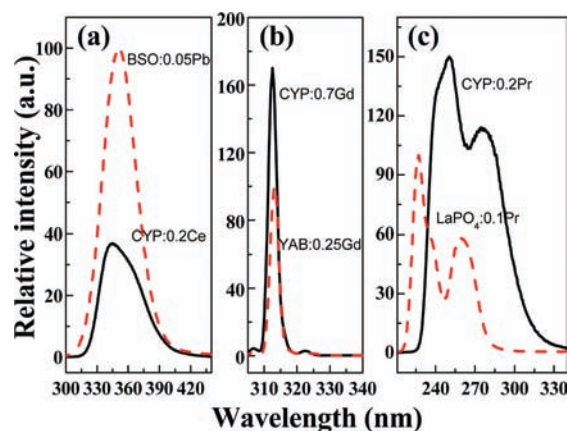


**Figure 6.** Comparison of the PL intensity of (a) UVA of $Ca_9Y(PO_4)_7:0.2Ce^{3+}$ (black solid line) and $BaSi_2O_5:0.05Pb^{2+}$ (red dashed line), (b) UVB of $Ca_9Y(PO4)_7:0.7Gd^{3+}$ (black solid line) and $YAl_3(BO_3)_4:0.25Gd^{3+}$ (red dashed line), and (c) UVC of $Ca_9Y(PO_4)_7:0.2Pr^{3+}$ (black solid line) and $LaPO_4:0.1Pr^{3+}$ (red dashed line) under 172 nm light excitation.

Figure 5 shows the concentration dependence of the relative PL intensity of $Ca_9Y(PO_4)_7:xCe^{3+}$, $Ca_9Y(PO_4)_7:yGd^{3+}$, and $Ca_9Y(PO_4)_7:zPr^{3+}$ phosphors under 172 nm excitation. Under 172 nm excitation, the relative emission intensity was observed to increase with the concentration of $Ce^{3+}$, $Gd^{3+}$, or $Pr^{3+}$ ($x < 0.2$, $y < 0.7$, and $z < 0.2$ mol) until the occurrence of concentration quenching. When the $Ce^{3+}$, $Gd^{3+}$, or $Pr^{3+}$ dopant concentration was higher than the optimal concentration ($x > 0.2$, $y > 0.7$, and $z > 0.2$ mol), the PL intensity was found to decrease with an increase in the $Ce^{3+}$, $Gd^{3+}$, or $Pr^{3+}$ dopant concentration. The optimal doping concentration of UVA-emitting $Ca_9Y(PO_4)_7:xCe^{3+}$ phosphors was found to be $x = 0.2$ mol, and the corresponding optimal doping concentrations of UVB-emitting $Ca_9Y(PO_4)_7:yGd^{3+}$ phosphors and UVC-emitting $Ca_9Y(PO_4)_7:zPr^{3+}$ phosphors were $y = 0.7$ mol and $z = 0.2$ mol, respectively. According to the percolation model,[20,21] concentration quenching of the compound can occur by two mechanisms: (1) the interaction between the activator ions, which results in energy reabsorption among neighboring activator ions in the rare-earth sublattice; (2) energy transfer from a percolating cluster of activator ions to killer centers.
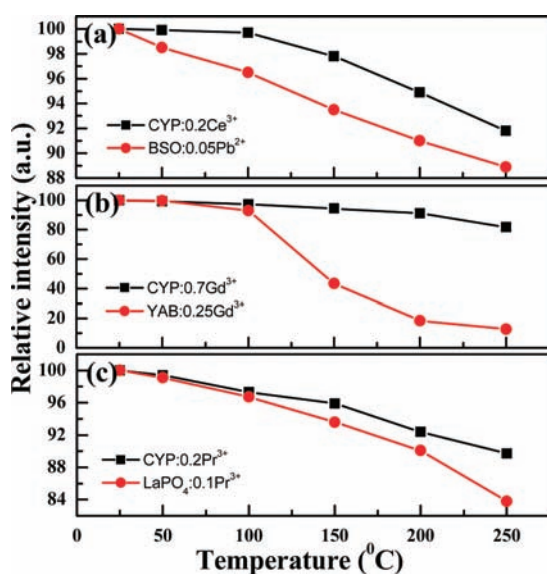
**Figure 7.** Temperature-dependent PL intensity of (a) $Ca_9Y(PO_4)_7:0.2Ce^{3+}$ and $BaSi_2O_5:0.05Pb^{2+}$, (b) $Ca_9Y(PO_4)_7:0.7Gd^{3+}$ and $YAl_3(BO_3)_4:0.25Gd^{3+}$, and (c) $Ca_9Y(PO_4)_7:0.2Pr^{3+}$ and $LaPO_4: 0.1Pr^{3+}$ phosphors.

**Table 1. Thermal Luminescence Quenching Data for $Ca_9Y(PO_4)_7:0.2Ce^{3+}$, $BaSi_2O_5:0.05Pb^{2+}$, $Ca_9Y(PO_4)_7:0.7Gd^{3+}$, $YAl_3(BO_3)_4:0.25Gd^{3+}$, $Ca_9Y(PO_4)_7:0.2Pr^{3+}$, and $LaPO_4:0.1Pr^{3+}$ Phosphors**

| sample | 25 °C | 50 °C | 100 °C | 150 °C | 200 °C | 250 °C |
|---|---|---|---|---|---|---|
| $CYP:0.2Ce^{3+}$ | 100 | 99.9 | 99.7 | 97.8 | 94.9 | 91.8 |
| $BSO:0.05Pb^{2+}$ | 100 | 98.5 | 96.5 | 93.5 | 91.0 | 88.9 |
| $CYP:0.7Gd^{3+}$ | 100 | 99.4 | 97.2 | 94.5 | 91.2 | 81.8 |
| $YAB:0.25Gd^{3+}$ | 100 | 99.7 | 93.1 | 43.4 | 18.4 | 12.7 |
| $CYP:0.2Pr^{3+}$ | 100 | 99.4 | 97.3 | 95.9 | 92.4 | 89.7 |
| $LaPO_4:0.1Pr^{3+}$ | 100 | 99.1 | 96.7 | 93.6 | 90.1 | 83.8 |

The PL intensity of the UVA emission of $Ca_9Y(PO_4)_7:0.2Ce^{3+}$ ($CYP:0.2Ce^{3+}$) and $BaSi_2O_5:0.05Pb^{2+}$ ($BSO:0.05Pb^{2+}$), that of the UVB of $Ca_9Y(PO_4)_7:0.7Gd^{3+}$ ($CYP:0.7Gd^{3+}$) and $YAl_3(BO_3)_4: 0.25Gd^{3+}$ ($YAB:0.25Gd^{3+}$), and that of the UVC of $Ca_9Y(PO_4)_7:0.2Pr^{3+}$ ($CYP:0.2Pr^{3+}$) and $LaPO_4:0.1Pr^{3+}$ phosphors under 172 nm excitation are compared in Figure 6. The emission spectra and optimal doping activator concentrations of the above UVR phosphors are excited at 172 nm. The PL spectra of the UVA-emitting $Ca_9Y(PO_4)_7:0.2Ce^{3+}$ and $BaSi_2O_5:0.05Pb^{2+}$ commodity phosphors show broad bands centered at 346 and 351 nm, respectively; these bands are attributed to the 5d $\rightarrow$ 4f transition of $Ce^{3+}$ and the $6s^16p^1 \rightarrow 6s^2$ transitions of $Pb^{2+}$ ions.[22] However, the emission intensity of the UVA-emitting $Ca_9Y(PO_4)_7:0.2Ce^{3+}$ is 0.3675 times that of the UVA emission of $BaSi_2O_5:0.05Pb^{2+}$. $Ca_9Y(PO_4)_7:0.7Gd^{3+}$ and $YAl_3(BO_3)_4:0.25Gd^{3+}$ phosphors show a strong 4f $\rightarrow$ 4f transition and a sharp UVB emission band at around 312 nm; this band is attributed to the $^6P_{7/2} \rightarrow {}^8S_{7/2}$ transition of $Gd^{3+}$ ions. The emission intensity of the UVB-emitting $Ca_9Y(PO_4)_7: 0.7Gd^{3+}$ is found to be 1.7 times that of the UVB emission of patented $YAl_3(BO_3)_4:0.25Gd^{3+}$. In the case of UVC-emitting phosphors, the PL spectra of $Ca_9Y(PO_4)_7:0.2Pr^{3+}$ show two

broad emission bands at 230−340 nm, centered at 250 and 275 nm. The PL spectra of $LaPO_4:0.1Pr^{3+}$ show two broad emission bands in the range of 210−280 nm, centered at 227 and 260 nm; these bands are attributed to the transition of $Pr^{3+}$ ions from 5d to 4f levels. The luminescence intensity of the UVC-emitting $Ca_9Y(PO_4)_7:0.2Pr^{3+}$ is 1.5 times that of the UVC emission of $LaPO_4:0.1Pr^{3+}$.

**3.3. Thermal Luminescence Quenching Properties.** Temperature dependence is an extremely important parameter for mercury-free fluorescent lamp applications. Figure 7 and Table 1 illustrate the temperature-dependent relative emission intensities of UVA-emitting $Ca_9Y(PO_4)_7:0.2Ce^{3+}$ and $BaSi_2O_5:0.05Pb^{2+}$ phosphors (excited at 225 nm and emission monitored at optimal wavelength), UVB-emitting $Ca_9Y(PO_4)_7:0.7Gd^{3+}$ and $YAl_3(BO_3)_4:0.25Gd^{3+}$ phosphors (excited at 274 nm and monitored at optimal wavelength), and UVC-emitting $Ca_9Y(PO_4)_7:0.2Pr^{3+}$ and $LaPO_4:0.1Pr^{3+}$ phosphors (excitation at 220 nm and monitored at optimal wavelength). The relative emission intensity decreases with an increase in temperature from 25 to 250 °C. We observed only a 5.1% decay of UVA-emitting $Ca_9Y(PO_4)_7:0.2Ce^{3+}$ (9% decay for $BaSi_2O_5:0.05Pb^{2+}$) phosphors at 200 °C, an 8.8% decay of UVB-emitting $Ca_9Y(PO_4)_7:0.7Gd^{3+}$ (81.6% decay for $YAl_3(BO_3)_4:0.25Gd^{3+}$) phosphors, and a 7.6% decay of UVC-emitting $Ca_9Y(PO_4)_7:0.2Pr^{3+}$ (9.9% decay for $LaPO_4:0.1Pr^{3+}$) phosphors, as shown in Figure 7a−c. These results show that UVR phosphors $Ca_9Y(PO_4)_7:0.2Ce^{3+}$, $Ca_9Y(PO_4)_7:0.7Gd^{3+}$, and $Ca_9Y(PO_4)_7:0.2Pr^{3+}$ have excellent thermal quenching stability than $BaSi_2O_5:0.05Pb^{2+}$, $YAl_3(BO_3)_4:0.25Gd^{3+}$, and $LaPO_4:0.1Pr^{3+}$ phosphors. Fabrication of mercury-free xenon excimer discharge lamps using UV-emitting $Ca_9Y(PO_4)_7:Ln^{3+}$ (Ln = Ce, Gd, Pr) phosphors described in this research is currently in progress and will be reported later.

# 4. CONCLUSIONS

Three series of new UVR phosphors $Ca_9Y(PO_4)_7:Ln^{3+}$ (Ln = Ce, Gd, Pr) were synthesized by a high-temperature solid-state method, and their photoluminescence spectra, emission efficiency, and thermal stability were investigated. Ultraviolet-emitting $Ca_9Y(PO_4)_7:Ln^{3+}$ (Ln = Ce, Gd, Pr) phosphors have high emission efficiency and decent thermal stability. Under 172 nm excitation, the luminescence intensity of the UVA-emitting $Ca_9Y(PO_4)_7:0.2Ce^{3+}$ was found to be 0.3675 times that of the UVA emission of $BaSi_2O_5:0.05Pb^{2+}$, the luminescence intensity of the UVB-emitting $Ca_9Y(PO_4)_7:0.7Gd^{3+}$ is 1.7 times that of the UVB emission of $YAl_3(BO_3)_4:0.25Gd^{3+}$, and the luminescence intensity of the UVC-emitting $Ca_9Y(PO_4)_7:0.2Pr^{3+}$ is 1.5 times that of the UVC emission of $LaPO_4:0.1Pr^{3+}$. The thermal stability of the above phosphors revealed that the extent of luminescence intensity decay was found to be only 9.2%, 18.2%, and 10.3% for $Ca_9Y(PO_4)_7:0.2Ce^{3+}$, $Ca_9Y(PO_4)_7:0.7Gd^{3+}$, and $Ca_9Y(PO_4)_7:0.2Pr^{3+}$ at 250 °C, respectively. These results indicate that $Ca_9Y(PO_4)_7:Ln^{3+}$ (Ln = Ce, Gd, Pr) phosphors may serve as promising UVR phosphors for use in xenon excimer discharge lamps.

# ■ AUTHOR INFORMATION

**Corresponding Author**
*E-mail: tmchen@mail.nctu.edu.tw.

## ■ REFERENCES

(1) Environmental Health Criteria 160, "Ultraviolet radiation", published under the International Labour Organization and the World Health Organization, 1994.

(2) Juestel, T. Recent Developments on UV Emitting Phosphors. *Phosphor Global Summit*, San Diego, CA, March 25th, 2010.

(3) Shie, J. L.; Lee, C. H.; Chiou, C. S.; Chang, C. T.; Chang, C. C.; Chang, C. Y. *J. Hazard. Mater.* **2008**, *155*, 164–172.

(4) Zamberk, P.; Velázquez, D.; Campos, M.; Hernanz, J. M.; Lázaro, P. *J. Eur. Acad. Dermatol. Venereol.* **2010**, *24*, 415–419.

(5) Nagira, T.; Narisawa, J.; Teruya, K.; Katakura, Y.; Shim, S. Y.; Kusumoto, K. I.; Tokumaru, S.; Tokumaru, K.; Barnes, D. W.; Shirahata, S. *Cytotechnology* **2002**, *40*, 125–137.

(6) Mercier, J.; Baka, M.; Reddy, B.; Corcuff, R.; Arul, J. *J. Am. Soc. Hortic. Sci.* **2006**, *126*, 128–133.

(7) Liu, J.; Stevens, C.; Khan, V. A.; Lu, J. Y.; Wilson, C. L.; Adeyeye, O.; Kabwe, M. K.; Pusey, P. L.; Chalutz, E.; Sultana, T.; Droby, S. *J. Food Prot.* **1993**, *56*, 868–872.

(8) Global Solar UV Index, "A Practical Guide", published under the World Health Organization, 2002.

(9) Tian, Z.; Liang, H.; Lin, H.; Su, Q.; Guo, B.; Zhang, G.; Fu, Y. *J. Solid State Chem.* **2006**, *179*, 1356–1362.

(10) Yokosawa, N.; Sato, G.; Nakazawa, E. *J. Electrochem. Soc.* **2003**, *150*, H197–H200.

(11) Okamoto, S.; Uchino, R.; Kobayashi, K.; Yamamoto, H. *J. Appl. Phys.* **2009**, *106*, 013522.

(12) Yuan, J. L.; Wang, J.; Xiong, D. B.; Zhao, J. T.; Fu, Y. B.; Zhang, G. B; Shi, C. S. *J. Lumin.* **2007**, *126*, 717–722.

(13) Folkerts, H. F.; Hamstra, M. A.; Blasse, G. *Chem. Phys. Lett.* **1995**, *246*, 135–138.

(14) JCPDS file no. 00-046-040.

(15) Gauthier, G.; Jobic, S.; Evain, M.; Koo, H. J.; Whangbo, M. H.; Fouassier, C.; Brec, R. *Chem. Mater.* **2003**, *15*, 828–837.

(16) Hölsä, J.; Lamminmäki, R. J.; Lastusaari, M.; Porcher, P. *J. Alloys Compd.* **2001**, *323−324*, 811–815.

(17) Liang, H.; Tao, Y.; Xu, J.; He, H.; Wu, H.; Chen, W.; Wang, S.; Su, Q. *J. Solid State Chem.* **2004**, *177*, 901–908.

(18) You, F.; Huang, S.; Meng, C.; Wang, D.; Xu, J.; Huang, Y.; Zhang, G. *J. Lumin.* **2007**, *122−123*, 58–61.

(19) Ustel, T. J.; Huppertz, P.; Mayr, W.; Wiechert, D. U. *J. Lumin.* **2004**, *106*, 225–233.

(20) Vyssotsy, V. A.; Gordon, S. B.; Frisch, H. L.; Hammersley, J. M. *Phys. Rev.* **1961**, *123*, 1566–1567.

(21) Kuo, T. W.; Huang, C. H.; Chen, T. M. *Opt. Express* **2010**, *18*, A231–A236.

(22) Paraschiva, M.; Nicoara, I.; Stef, M.; Bunoiu, O. M. *Acta Phys. Pol., A* **2010**, *117*, 466–470.

6556

dx.doi.org/10.1021/ic2001877 |*Inorg. Chem.* 2011, 50, 6552–6556